

Development of a versatile lidar system based on passively Q-switched Nd: YAG laser for monitoring aerosols and cirrus clouds in the atmosphere

Hai Van Bui^{1,†}, Trung Van Dinh², Bao Thi Thanh Nguyen², Oanh Thi Kim Vu²,
Tu Xuan Nguyen², Tiep Viet Phung², Van Thi Khanh Nguyen², Bang Dong Pham³,
Tien Minh Pham⁴, Thieu Van Nguyen⁵, Thanh Van Hoang⁶,
Dien Tran Nguyen⁷ and Anh Ngoc Bao Phung⁸

¹*Le Quy Don Technical University, 236 Hoang Quoc Viet, Hanoi, Vietnam*

²*Institute of Physics, Vietnam Academy of Science and Technology,
10 Dao Tan, Ba Dinh, Hanoi 11108, Vietnam*

³*Graduate University of Science and Technology,
Vietnam Academy of Science and Technology, 18 Hoang Quoc Viet, Cau Giay, Hanoi, Vietnam*

⁴*Department of Artificial Intelligence and Data Science, Thuyloi University - Southern Campus,
An Thanh, Thuan An, Binh Duong, Vietnam*

⁵*Department of Science and Technology of Quang Binh, Dong Hoi, Vietnam*

⁶*VNU University of Science, 334 Nguyen Trai, Thanh Xuan, Hanoi, Vietnam*

⁷*Institute of Environmental Technology, Vietnam Academy of Science and Technology,
18 Hoang Quoc Viet, Cau Giay, Hanoi, Vietnam*

⁸*Institute of Human Geography, 18 Hoang Quoc Viet, Cau Giay, Hanoi, Vietnam*

E-mail: [†]bvhaihsh@lqdtu.edu.vn

Received 12 October 2023; Accepted for publication 28 December 2023

Published 05 February 2024

Abstract. *In this paper, we present an in-house flexible and portable lidar system integrating an inexpensive, passively Q-switched laser Nd: YAG and a detection module operating in both analog and photon counting mode. This system is designed to study the atmospheric boundary layer (BL) and cirrus clouds (CC). The passively Q-switched Nd:YAG pulsed laser, operating at a second-harmonic generation (SHG) wavelength of 532 nm, features a pulse energy up to 200 mJ, a repetition rate of 1 Hz to 15 Hz, and a pulse duration of 15 ns. Our lidar system is designed to provide multi-angle measurements up to 25 km. The multi-angle capability allows direct determination of the overlap function, characterizing the system by measuring the horizontal lidar signal.*

This lidar system is used to monitor the boundary layer and cirrus clouds over several locations in Hanoi, Quang Binh, Da Nang and Ho Chi Minh city. From the measurements, we derive key properties such as the height, thickness, and optical depth of the Earth's surface aerosol layer and cirrus clouds. We have demonstrated that such a lidar system is very useful for aerosol research and the study of high cirrus clouds.

Keywords: passive Q-switch laser; aerosol; cirrus cloud; optical depth; lidar ratio.

Classification numbers: 42.60.Gd; 42.68.Ge; 42.79.Qx; 92.60.Mt.

1. Introduction

Aerosols and high-altitude clouds are important components of the atmosphere. They are widely distributed over urban areas, countryside, mountains, forests, deserts, oceans, ice, and all other ecosystems. Aerosols and cirrus clouds contribute significantly to the energy balance of the Earth through the absorption and scattering of solar radiation. As a result, they also play a pivotal role in the meteorological process, weather variations, climate change, and air quality [1–6]. Understanding the structure of aerosols in the planetary boundary layer and high cloud layers has become a key focus for scientists aiming to monitor, analyze, characterize, and quantify these atmospheric elements. Over the past several decades, numerous methods and techniques have been developed for researching these objects. Among high-resolution spectral optical techniques, lidar has emerged as a superior tool in atmospheric and environmental studies [7–10].

Over the past decade, a multi-channels lidar system has been developed and operated for continuously monitoring atmosphere at a station in 18 Hoang Quoc Viet street, Cau Giay, Hanoi, Vietnam. Our lidar group has reported impressive results in articles [11–14], which detail the objectives of using lidar technology, as well as its application in researching the physical properties and distribution of the boundary layer and cirrus clouds over Hanoi (21.03°N, 105.85°E).

Vietnam, a developing country with a latitudinal range from 23°09'09" in Ha Giang to 10°17'14" in Phu Quoc, faces significant environmental pollution challenges along its western Pacific coast. In response, we aim to develop a versatile mini lidar system for researching aerosol at various locations across Vietnam [15–19]. Therefore, establishing a network of atmospheric research lidar stations throughout the country is both scientifically significant and necessary.

A lidar system consists of two main components: a transmitter block comprising a high-power pulsed laser and a receiver block contains a high-sensitivity photodetector. For high-altitude atmospheric studies, the transmitter typically uses a durable, high-power laser, with commercial pulsed Nd:YAG lasers being the ideal choice. However, their bulkiness and high cost pose great challenges for lidar system development in conventional laboratories, hindering continuous atmospheric monitoring during a long period. This has led to the studies of numerous groups in the world to design alternative transmitters in lidar systems. High power diode lasers emitting at various wavelengths (450 nm, 808 nm, 905 nm, 1550 nm, etc.) have been employed in lidar systems [20–24]. Even pulsed LEDs have been tested as an emitter for lidar systems to measure the boundary layer [25]. Yet, due to their limited emitting power, systems based on diode lasers and LEDs are typically only suitable for near-range monitoring. In this context, the flash-lamp pumped passively Q-switched Nd:YAG, operating at both 1064 nm and 532 nm, presents a promising and flexible solution, offering robustness and compactness.

In this work, we report the design of the multi-angles lidar system based on the passively Q-switched Nd:YAG laser and some initial measurements monitoring the main properties of boundary and cirrus layers in various provinces in Vietnam. The high-power multi-angles lidar system enables the development of atmospheric and environmental studies in three-dimensional space, with a range extending up to 20 kilometers. We have utilized this system to monitor aerosol boundary layer and high-latitude cirrus clouds, and to analyze the micro-properties such as height, thickness, optical depth, and lidar ratio.

2. System description

2.1. Mini transmitter

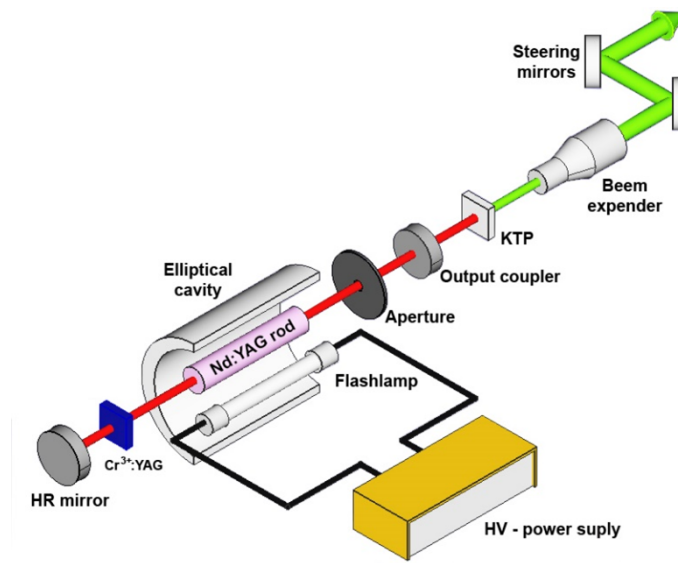


Fig. 1. Schematics of a passively Q-switched Nd: YAG laser used in our lidar system.

Our laser is specifically designed and built for integration into a multi-angle lidar system, capable of probing the atmosphere over long distances and at various angles. A schematic diagram of the laser cavity is shown in Fig. 1. The lidar system's transmitter is based on a high-power pulsed laser, utilizing a Q-switched Cr³⁺: YAG crystal saturable absorber with the repetition rate tunable from 1 Hz to 15 Hz. This depends on the pumped rate of flashligh operating with the laser pulse duration of 15 ns. The length of Fabry – Perot optical cavity is expanded to 700 mm to enhance the spatial coherence of the laser beam. The quality of the laser beam's cross-mode is modified by using an aperture that adjusts the size of the active media square excited in the Nd: YAG crystal rod. The divergence of the laser beam reaches approximately 1 mrad when the diameter of the aperture is fixed at 3 mm. The F-P cavity consists of two mirrors: a 100% reflective mirror and a 40% transmissive mirror serving as the output coupler. A Nd:YAG cylinder crystal rod with 5 mm of diameter, 100 mm of length that is placed parallel to a flash lamp operated at high voltage from 500 V to 1000 V. Cavity is totally closed and cooled with pure water flowed by

Chiller CW-3000 with a pump power of 80 W. The cooler ensures the operating temperature does not exceed the ambient temperature by more than 5 degrees. The laser beam is expanded by a 3X beam expander before being transmitted vertically into the atmosphere by two steering mirrors.

A second harmonic generator is a KTP crystal (KTiOPO_3) with $6 \times 6 \times 3$ mm in size to generate a pulse laser at wavelength of 532 nm. Under stable operation condition, and with a 900V voltage supplied to the flash lamp, the laser pulse at the 532 nm wavelength can achieve an energy of approximately 10 mJ per pulse. This is at a repetition rate of 5 Hz and with a pulse duration of 15 ns. With the power of this laser transmitter, the lidar system in photon counting mode detects the backscattered signal from the tropopause at 20 km altitude by using a gated PMT detector. A more detailed analysis of the cloud survey signal will be provided in [Subsection 5.2](#). Using photon counting mode we could reach the tropopause and detect cirrus clouds. The operation of the laser module is simple and robust, making it suitable for portable lidar systems.

Table 1. Technical specifications of Brilliant laser series made by Quantel and the transmitter in the multi-angle lidar system.

Transmitter		
<i>Properties</i>	<i>Brilliant Quantel -France</i>	<i>In-house developed laser</i>
Cavity type	super gaussian resonator	Fabry-Perot cavity length - 700 mm
<i>Active medium</i>		
Type of crystal	Nd: YAG	Nd: YAG
Diameter	8 mm	5 mm
Length	150 mm	100 mm
<i>Second harmonic generator</i>		
Type of crystal	KDP	KTP - KTiOPO_3
Size of crystal (LxHxW)	20x10x10 mm	$3 \times 6 \times 6$ mm
<i>Specifications</i>		
Wavelength	532 nm	532 nm
Repetition rate (Hz)	10 Hz	1-15 Hz
Pulse energy (mJ)	0 - 180 mJ	10 - 450 mJ at 5 Hz & S.Vol. 900 V
Pulse duration (ns)	5 ns	15 ns
Divergence of laser beam	0.5 mrad	1 mrad
Power (V)	110 - 240 V, 10 A, 50 Hz	110 - 240 V, 10 A, 50 Hz
<i>Integrated Cooling and Electronics</i>		
Size ($L \times W \times H$)	$720 \times 340 \times 500$ mm	$570 \times 350 \times 470$ mm
Weight	14 kg	3.8 kg
Mass of Nd: YAG laser (kg)	7.1 kg	3.6 kg
Optical laser head $L \times H \times W$ (mm)	$627 \times 136 \times 80$ mm	$800 \times 200 \times 250$ mm

With lightweight and a simple resonant cavity structure, users can easily assemble, disassemble, and relocate this system. The compactness and ease of assembly are prominent advantages of our mechanical-optical system. However, the system's overall functionalities and observational capabilities are fully comparable to the lidar systems using industrial laser transmitter from the Brilliant Quantel–France company in monitoring the boundary layer and cirrus clouds. The specifications of our laser transmitter, designed for this lidar system, are listed in Table 1 alongside those of the industrial-grade laser transmitter from the Brilliant company. The primary distinction lies in the active design of the mechanical dimensions of our 2W transmitter, which enables its coaxial attachment to the optical receiver, facilitating measurements at various angles.

2.2. Receiving module

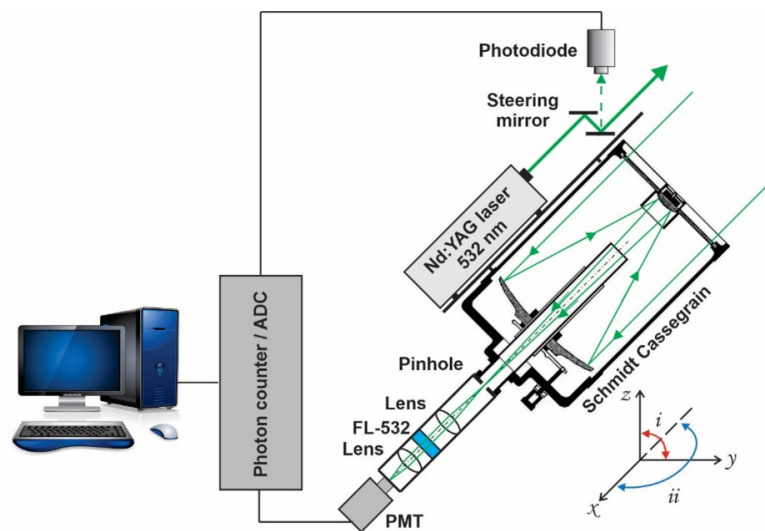


Fig. 2. The schematic diagram of the versatile lidar system.

The backscattering photons are collected by a Schmidt-Cassegrain telescope of 20 cm in diameter ($f/D = 10$), mounted on two synchronized parallel axes. To reduce the background noise, the field of view of the telescope is limited to below 1.5 mrad during the measurement time. This is achieved by employing a 3 mm diameter pinhole (field stop) at the telescope's focal plane, as illustrated in figure 2. Furthermore, we use a narrow band interference filter (Thorlabs) centered at 532 nm with a bandwidth of 1 nm to reject the ground noise. The signal is focused on the photon detector which could be operated in either photon counting mode or analog mode. In standard photon counting mode, a PMT R7400U-20 head is used (Hamamatsu, Japan) for near field and an electrically gated PMT R7400U for the high cirrus layers. In the daytime, the lidar is operated in analog mode with the detector used such as a PMT H6780-20 head (Hamamatsu, Japan). Our lidar system is flexible for monitoring the high cirrus clouds in both day and night. Analog and photon-counting modes can be easily switched on/off by software. An analog to digital converter is based on the commonly available USB digital oscilloscope (Picoscope 5024 – Picotech of UK) with a bandwidth of 250 MHz. A photodiode is used to detect the laser pulses before shooting into the atmosphere and mark the start point of data acquisition for each profile. The detected

photons are accumulated over a predefined number of laser pulses and saved for further analysis. The software is written in Labview language and easily contacts the received module with the computer. However, for photon mode, we have developed two photon counting detectors: one for monitoring aerosols in the near field using the PMT R7400U-20 head, and another for tracking high cirrus clouds with an electronically gated PMT R7400U head. The gated PMT is a crucial component for enhancing the signal-to-noise ratio and improving detection of weak backscattering signals [12].

3. Lidar data analysis

The basic lidar equation presents a relationship between backscattered signal intensity verse the range z . That is shown in Ref [7, Eq. (1)]:

$$P(z) = P_{\text{Laser}} \cdot O(z) \cdot C \cdot Z^{-2} \cdot \beta(z) \cdot \exp \left[-2 \int_0^z \sigma(z) dz \right]. \quad (1)$$

In this equation, $\beta(z) = \beta_a(z) + \beta_m(z)$, $\beta_a(z)$ and $\beta_m(z)$ are the backscatter coefficients of aerosol particles and air molecules at range z , respectively. P_{Laser} is the energy of a laser pulse. $O(z)$ is the spatial featured overlap function of the lidar system. C is the calibration constant of our lidar system. $P(z)$ is the lidar return signal received by from the scattering volume at range of z . $\sigma(z)$ is known as total extinction of the air, $\sigma(z) = \sigma_a(z) + \sigma_m(z)$, $\sigma_a(z)$ and $\sigma_m(z)$ are the extinction of aerosols and molecules, respectively.

$$T_a(z) = \exp \left[- \int_0^z \sigma_a(z) dz \right], \quad (2)$$

$$T_m(z) = \exp \left[- \int_0^z \sigma_m(z) dz \right], \quad (3)$$

where $T_a(z)$ and $T_m(z)$ represent the transmittance of aerosols and molecules, respectively, at a high range z . The ratio between molecular extinction σ_m and their backscatter coefficient β_m is given by $\frac{\sigma_m}{\beta_m} \approx 8 \frac{\pi}{3}$ from Rayleigh-scattering theory [7]. The corresponding ratio for aerosol particles is generally known as lidar ratio, $S_a = \frac{\sigma_a}{\beta_a}$, derived by using the transmission method [26–28]. In our data analysis, the measured signals are subtracted from baseline and range-corrected averaged to improve signal to noise ratio. From the measured data, we can determine the top height of the aerosol layer, the base and top of cirrus cloud and optical depth of these layers. An important parameter of these cirrus clouds is optical depth τ_{to} . Optical depth is determined by an equation in single scattering approximation, as follows:

$$\tau_{\text{to}} = \int_{z_{\text{base}}}^{z_{\text{top}}} \sigma(z') \cdot dz' = \int_{z_{\text{base}}}^{z_{\text{top}}} S_c(z') \cdot \beta(z') \cdot dz' = - \ln \left(\frac{P_{\text{top}} \cdot z_{\text{top}}^2}{P_{\text{base}} \cdot z_{\text{base}}^2} \right)^{\frac{1}{2}}, \quad (4)$$

where z_{base} and z_{top} represent the base and top heights of a layer of cirrus cloud respectively. z_{base} and z_{top} are determined using the threshold method as described in [12]. The geometrical thickness of the cirrus cloud is the difference between its base and top heights. In the threshold method, the starting point is chosen in the clear atmosphere and then marched upward or downward for determining the base and top point of the tracking layer, at which the intensity significantly increase

in the lidar signals (about five times the standard deviation of the back signal from molecular scattering).

The mean lidar ratio in one cloud layer is computed by integrating the extinction and backscatter coefficients across the extent of the cloud layer, from the base to the top height, as shown in Eq. (5). In this framework, we can calculate the backscatter coefficient profile using Klett-Fernald method [29–32].

$$S_c = \frac{\int_{z_{\text{base}}}^{z_{\text{top}}} \sigma_c(z) \cdot dz}{\int_{z_{\text{base}}}^{z_{\text{top}}} \beta_c(z) \cdot dz} \quad (5)$$

The blind zone of our lidar system is under 650 m, which primarily determined by the lidar system's geometrical factor. This parameter limits significantly the range of a lidar system, as represented in the system's overlap function. In Hanoi, the top height of the boundary layer is often observed to be below 1.3 km [33]. Consequently, overlap function becomes an important parameter in analyzing the characteristics of the boundary aerosol layer. In this issue, we introduce an experimental method to define the geometrical form factor of our elevation-scanning lidar system.

We assume that in the entire horizontal range, the medium is homogeneous [8, 19, 34, 35]. The backscatter coefficient β and extinction coefficient ρ are considered constant in all range of lidar signals. To further analyze this, we take the natural logarithm of both sides of Eq. (1):

$$\begin{aligned} S(z) &= \ln(P(z) \cdot z^2) \\ &= \ln(O(z)) + \ln(P_{\text{Laser}} \cdot C) + \ln[\beta_a(z) + \beta_m(z)] - 2 \int_0^z (\sigma_a(z) + \sigma_m(z)) \cdot dz. \end{aligned} \quad (6)$$

In horizontal path, $\ln(P_{\text{Laser}} \cdot C) + \ln[\beta_a(z) + \beta_m(z)]$ is unchanged, $\ln(P_{\text{Laser}} \cdot C) + 2 \int_0^z (\sigma_a(z) + \sigma_m(z)) \cdot dz$ is a linear rule. Eq. (6) is rewritten in short form of the following equation

$$\ln(P(z) \cdot z^2) - \ln(O(z)) = a \cdot z + b, \quad (7)$$

where a and b represent the coefficients of the first-degree linear equation fitted according to Eq.(7). For a long range of view, the overlap function approaches 1, indicating that the laser beam is completely in the field of view of the telescope. In this way, we can define the geometrical factor $O(v)$ of the lidar system, as detailed in the following equation

$$O(z) = \exp[\ln(P(z) \cdot z^2) - (a \cdot z + b)] \quad (8)$$

Moreover, we utilize the data of MSIS-E-90 model, an empirical model of the temperature and composition of the atmosphere at heights between 0 km and 700 km [11, 14, 29], to directly calculate the optical depth of molecular in the range of the clean atmospheric layer. Typically, the range of clean air is chosen to be between 7 km and 20 km. The back scattering coefficient of molecules is showed in the following equation [2, 7]:

$$\beta_\pi^R = N_m \cdot 5.45 \left(\frac{550}{\lambda} \right)^4 \cdot 10^{-28} \text{ cm}^{-1} \text{ sr}^{-1} \quad (9)$$

Optical depth of molecules is specified by this equation 10 with lidar ratio of the molecules as $S_m = \frac{8 \cdot \pi}{3}$ [7].

$$\tau_m = \int_0^z S_m \cdot \beta_\pi^R \cdot dz \quad (10)$$

By this way, the transmittance of aerosols τ_a can be defined by subtracting τ_{to} from τ_m .

4. Determination of overlap function

In this section, we demonstrate an experimental method to determine the Geometrical Form Factor (GFF), by analyzing the lidar signal in the horizontal direction. Each lidar system has a unique GFF, which characterizes for the construction of the system [19, 36].

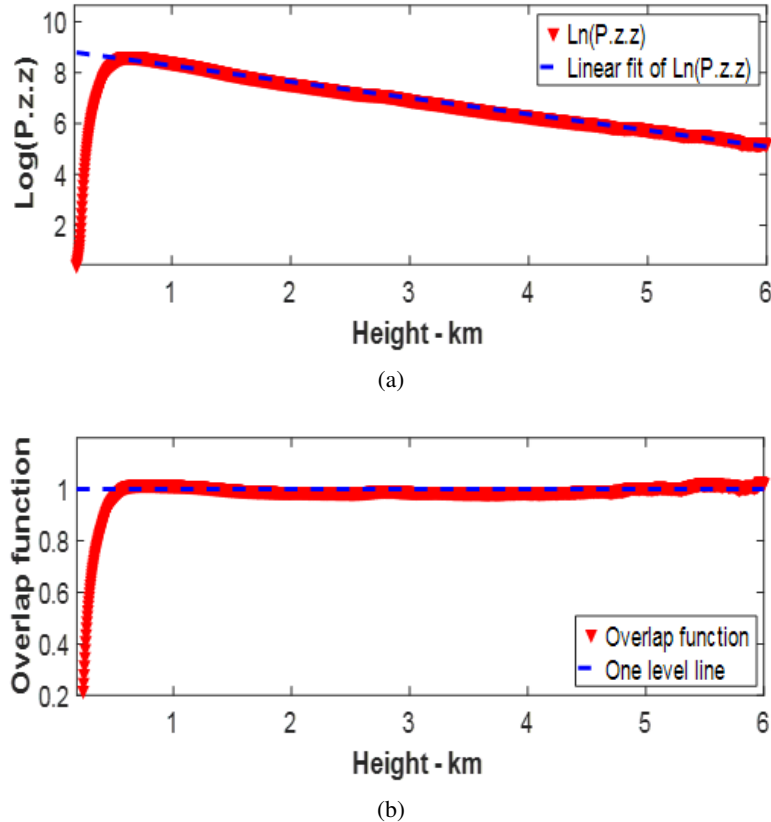


Fig. 3. a) Range corrected signal in horizontal direction. b) Overlap function (GFF) of the lidar system characterizing the geometrical factor received from the backscattering signal in horizontal direction on case of 17th January 2021, as shown in Eq. (7).

The overlap function defines the coupling of spatial factors between laser beam and field of view of the receiver (telescope) as a function of height [37]. GFF characterizes the spatial overlap between the transmitter and the field of view of the receiver. This depends on the field of view of the telescope, divergence of the laser beam as well as the distance between the optical axis of laser beam and axis of the receiver. A coaxial mode lidar system, used for continuous monitoring of the near aerosol layer, simplifies the alignment process during scanning. However, in a coaxial mode lidar scanning system, with the laser beam fixed at the center of the telescope, the backscatter signal can cause strong background noise in the detector, leading to signal interference due to noise. In long time operation of this lidar system, the coaxial mode can damage the PMT.

Figure 3a shows the linear function $y = -0.64.x + 8.91$, fitted to $\lg(P.z.z)$ (natural logarithm of range corrected signal - $P.z.z$) versus height in the horizontal direction. The dashed line shows the relationship of $\lg(\text{range-corrected signal})$ depending on distance in the optical homogeneous medium, analogous to the backscattering signal in the horizontal direction.

In our versatile lidar system, we establish coaxial optical configuration between telescope receiver and laser beam of transmitter. The passive laser is mounted on telescope of MEADE company. In this setup, the overlap function is less than one within the range below 632 meters. In monitoring the properties of the near field aerosol layer, the overlap function is a critical parameter in the broadening backscattering signals. In this work, we demonstrate an experimental method to extend the detecting range of GFF from 632 m down to 180 m by using multi-axis lidar system [19].

5. Lidar measurements

5.1. Monitoring boundary layer

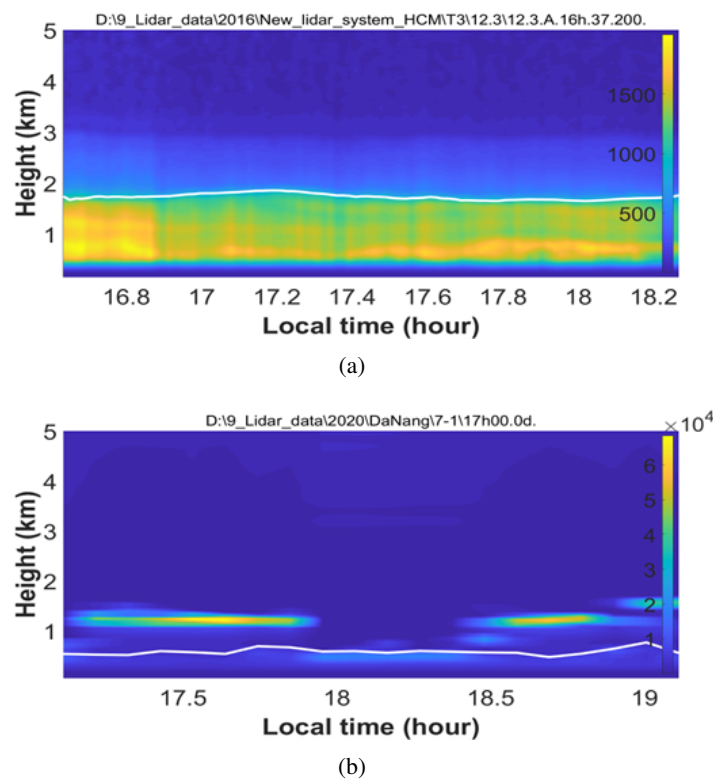


Fig. 4. The observation of the boundary layer in Ho Chi Minh city, Da Nang city and Hanoi city monitored by our mobile lidar system.

Figure 4a presents a quick look at the boundary layer over Ho-Chi-Minh city on March 12th, 2016, from 16:40 to 17:10. In this case, the boundary layer is at 1.729 km altitude, which is

higher compared to other locations such as those shown in Figs. 4b, 4c. The increased top height of the boundary layer in Ho Chi Minh city is attributed to intensified convection processes under a stronger radiant budget, as indicated by the average temperature of the day being 36°C, in clear atmospheric conditions.

Figures 4b and 4c show two examples of the same observation of boundary layer in Danang and Hanoi in January March 2020 and February 2022, respectively. The top heights of the boundary layer are 584 m and 303 m, respectively. In both cases, we observe the presence of a cloud layer near the surface under 2 kilometers.

The altitude of the surface boundary layer is directly related to the level of air pollution, serving as an atmospheric parameter reflecting the temperature background and the process of total radiation retention. Variations in the altitude of the surface atmospheric layer indicate changes in the convective process and the movement of air masses throughout the day. Observations of the near-surface layer using lidar techniques are frequently conducted at atmospheric and environmental research centers over the world [1, 5, 10, 20]. In recent years, alongside remote sensing techniques using balloons, lidar technology has also been employed and has yielded highly valuable research data [11–14].

5.2. Observations of cirrus clouds

5.2.1. Macro-optical properties

The aerosol layer over 6 km known as cirrus clouds in troposphere is the important component in the atmosphere of the earth. This is the main power budget of the sun radiation and makes two opposite effects known as greenhouse and albedo effects [2, 14]. These phenomena are major contributors to the rising temperatures of our planet. Therefore, cirrus clouds are the main objects of detailed research interest in the fields of atmospheric science, astronomy, aviation, and the environment. Apart from conventional visual surveys and aerial devices, lidar stands as an efficient technique with high spatial and temporal resolution. The lidar technique is particularly effective for determining macroscopic parameters of cirrus clouds, such as their altitude distribution, top height, base height, and overall cloud layer thickness.

5.2.2. Micro-optical properties

Besides the macroscopic optical characteristics, the important microphysical optical features of Cirrus clouds that are usually surveyed include optical depth, polarization, extinction coefficient, backscatter coefficient, and lidar ratio [2, 7, 11, 13, 26, 27]. In this work, we use a gated PMT module in counting mode in nighttime, the weak signals are received from the height above 25 km in the atmosphere. Fig. 6 showed a case of a thick cirrus cloud, the back signals are averaged in 15 minutes in counting mode by gated PMT. We can derive the height of base and top of cirrus layer at 13.5 km and 17.0 km using threshold method [14]. From this data, we calculate an optical depth and averaged lidar ratio of this cirrus cloud layer to be 0.21 and 39, respectively. In this study, we utilize the Ferlnald - Klett algorithm based on multiple scattering theory, applied to the backscattered data captured by the measurement system, to determine the optical depth and characteristic lidar ratios of this cirrus cloud layer [26–28]. All data from this lidar system, including a study on the macro properties of cirrus clouds over Hanoi, are presented in Ref. [14].

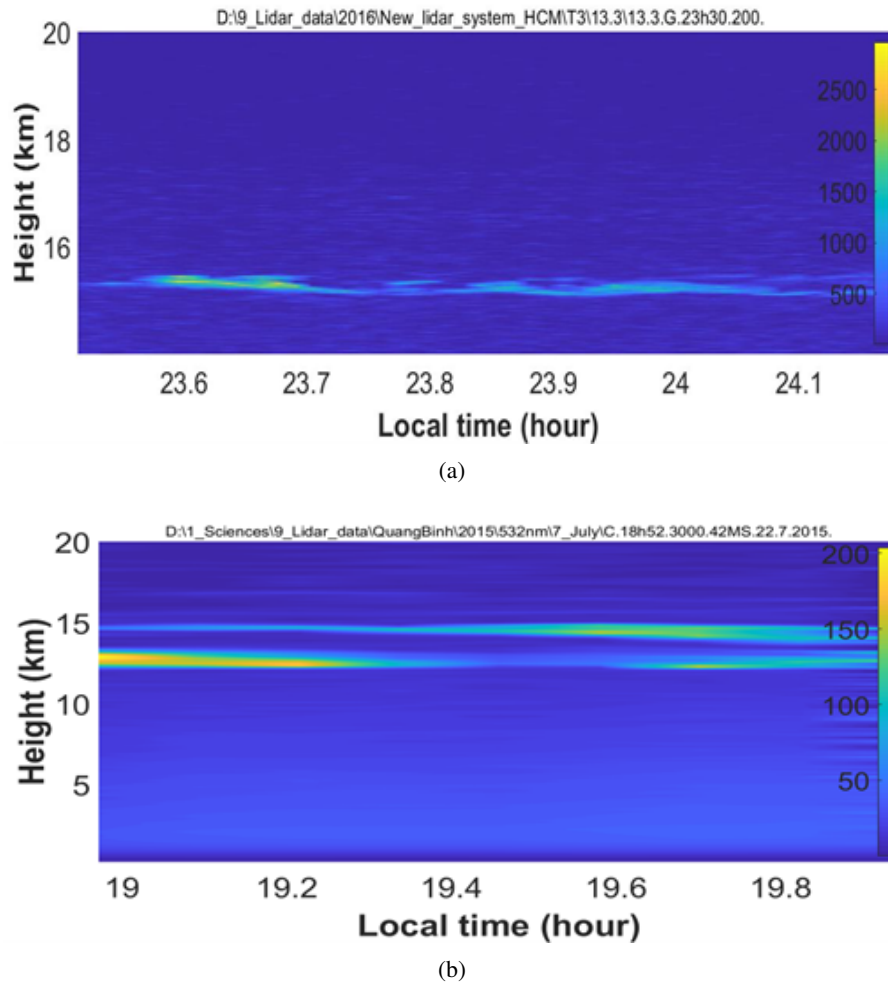


Fig. 5. An example of monitoring a thin cirrus cloud in Ho Chi Minh city and Quang Binh province used this lidar system.

6. Conclusion

We have designed and developed a versatile lidar system based on passively Q-switched Nd:YAG laser monitoring aerosol and cirrus clouds in the atmosphere at wavelength of 532 nm with both analog mode and photon counting mode. Which is useful in understanding their physical properties, temporal and spatial variability. This lidar system is designed with small size, light weight and suitable for installation in various vehicles and therefore will be handy for monitoring atmospheric pollution.

The continuous monitoring of the versatile lidar system will gather information for researching pollution episodes. Such data will be valuable for understanding the characteristics of pollution transport, which combines with conventional point-sampling data to serve better for

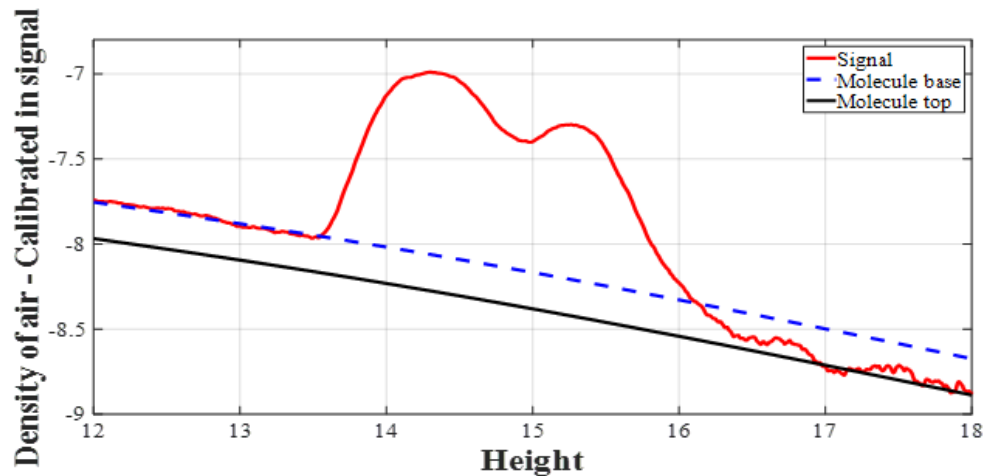


Fig. 6. A profile of elastic signal in vertical direction shows clearly base height at 13.5 km and top height at 17.0 km of a cirrus cloud layer.

studies on large spatial scale. The capability to measure from multiple angles expands the observational area of the lidar system in the near field. It conducts optical depth measurements of the surrounding atmosphere.

Acknowledgements

This research was funded by the Vietnam Academy of Science and Technology under Project No. VAST01.03/22-23.

References

- [1] W. Bach, *Global air pollution and climatic change*, *Rev. Geophys.* **14** (1976) 429.
- [2] S. Twomey, *Aerosols, clouds and radiation*, *Atmos. Environ. A* **25** (1991) 2435.
- [3] Y. J. Kaufman, D. Tanré and O. Boucher, *A satellite view of aerosols in the climate system*, *Nature* **419** (2002) 215.
- [4] I. Mattis, A. Ansmann, D. Müller, U. Wandinger and D. Althausen, *Multiyear aerosol observations with dual-wavelength raman lidar in the framework of earlinet*, *Journal of Geophysical Research: Atmospheres* **109** (2004) D13203.
- [5] M. O. Andreae, C. D. Jones and P. M. Cox, *Strong present-day aerosol cooling implies a hot future*, *Nature* **435** (2005) 1187.
- [6] H. K.-F. Zhang Ren-Jian and S. Zhen-Xing, *The role of aerosol in climate change, the environment, and human health*, *Atmospheric and Oceanic Science Letters* **5** (2012) 156.
- [7] R. Measures, *Laser Remote Sensing: Fundamentals and Applications*. Krieger Publishing Company, 1992.
- [8] K. Fredriksson, B. Galle, K. Nyström and S. Svanberg, *Mobile lidar system for environmental probing*, *Appl. Opt.* **20** (1981) 4181.
- [9] T. Murayama, N. Sugimoto, I. Uno, K. Kinoshita, K. Aoki, N. Hagiwara *et al.*, *Ground-based network observation of asian dust events of april 1998 in east asia*, *J. Geophys. Res. Atmos.* **106** (2001) 18345.
- [10] A. Ansmann, J. Bösenberg, A. Chaikovsky, A. Comerón, S. Eckhardt, R. Eixmann *et al.*, *Long-range transport of saharan dust to northern europe: The 11–16 october 2001 outbreak observed with earlinet*, *J. Geophys. Res. Atmos.* **108** (2003) 4783.

- [11] B. V. Hai, D. V. Trung, N. X. Tuan, D. D. Thang and N. T. Binh, *Monitoring cirrus cloud and tropopause height over hanoi using a compact lidar system*, *Comm. Phys.* **22** (2013) 357.
- [12] T. N. Xuan, H. B. Van and T. V. Dinh, *Normally off-gated photomultiplier tube module in photon-counting mode for use in light detection and ranging measurements*, *J. Appl. Remote Sens.* **8** (2014) 083536.
- [13] T. Pham Minh, T. Nguyen Xuan, T. Dinh Van, M. Le Duy and H. Bui Van, *Depolarization property of cirrus clouds over hanoi*, *Comm. Phys.* **27** (2017) 339.
- [14] H. V. Bui, M. D. Le, T. V. Dinh, T. X. Nguyen, T. M. Pham, H. N. Tran *et al.*, *Optical and geometrical properties of cirrus clouds from lidar measurements above Hanoi, Vietnam*, *J. Appl. Remote Sens.* **13** (2019) 034523.
- [15] S. D. Mayor and S. M. Spuler, *Raman-shifted eye-safe aerosol lidar*, *Appl. Opt.* **43** (2004) 3915.
- [16] M. Radlach, A. Behrendt and V. Wulfmeyer, *Scanning rotational raman lidar at 355 nm for the measurement of tropospheric temperature fields*, *Atmos. Chem. Phys.* **8** (2008) 159.
- [17] A. Behrendt, V. Wulfmeyer, A. Riede, G. Wagner, S. Pal, H. Bauer *et al.*, *Three-dimensional observations of atmospheric humidity with a scanning differential absorption Lidar*, *Proceedings Volume 7475, Remote Sensing of Clouds and the Atmosphere XIV* **7475** (2009) 74750L.
- [18] A. Behrendt, S. Pal, V. Wulfmeyer, Álvaro M. Valdebenito B. and G. Lammel, *A novel approach for the characterization of transport and optical properties of aerosol particles near sources – part i: Measurement of particle backscatter coefficient maps with a scanning uv lidar*, *Atmospheric Environment* **45** (2011) 2795.
- [19] C.-W. Chiang, S. K. Das, H.-W. Chiang, J.-B. Nee, S.-H. Sun, S.-W. Chen *et al.*, *A new mobile and portable scanning lidar for profiling the lower troposphere*, *Geoscientific Instrumentation, Methods and Data Systems* **4** (2015) 35.
- [20] C. Münkler and R. Roininen, *Automatic monitoring of boundary layer structures with ceilometers*, *Vaisala News* **184** (2010) .
- [21] G. Tsaknakis, A. Papayannis, P. Kokkalis, V. Amiridis, H. Kambezidis, R. Mamouri *et al.*, *Inter-comparison of lidar and ceilometer retrievals for aerosol and planetary boundary layer profiling over athens, greece*, *Atmos. Meas. Tech.* **4** (2011) 1261.
- [22] L. Mei and M. Brydegaard, *Atmospheric aerosol monitoring by an elastic scheidpflug lidar system*, *Opt. Express* **23** (2015) A1613.
- [23] L. Mei, P. Guan and Z. Kong, *Remote sensing of atmospheric no₂ by employing the continuous-wave differential absorption lidar technique*, *Opt. Express* **25** (2017) A953.
- [24] S. M. Pershin, A. L. Sobisevich, M. Y. Grishin, V. V. Gravirov, V. A. Zavozin, V. V. Kuzminov *et al.*, *Volcanic activity monitoring by unique lidar based on a diode laser*, *Laser Physics Letters* **17** (2020) 115607.
- [25] W. Zhong, J. Liu, D. Hua, S. Guo, K. Yan and C. Zhang, *White led light source radar system for multi-wavelength remote sensing measurement of atmospheric aerosols*, *Appl. Opt.* **58** (2019) 8542.
- [26] S. A. Young, *Analysis of lidar backscatter profiles in optically thin clouds*, *Appl. Opt.* **34** (1995) 7019.
- [27] W.-N. Chen, C.-W. Chiang and J.-B. Nee, *Lidar ratio and depolarization ratio for cirrus clouds*, *Appl. Opt.* **41** (2002) 6470.
- [28] C.-W. Chiang, S. K. Das and J.-B. Nee, *An iterative calculation to derive extinction-to-backscatter ratio based on lidar measurements*, *J. Quant. Spectrosc. Radiat. Transf.* **109** (2008) 1187.
- [29] F. G. Fernald, *Analysis of atmospheric lidar observations: some comments*, *Appl. Opt.* **23** (1984) 652.
- [30] J. D. Klett, *Stable analytical inversion solution for processing lidar returns*, *Appl. Opt.* **20** (1981) 211.
- [31] E. Giannakaki, D. S. Balis, V. Amiridis and S. Kazadzis, *Optical and geometrical characteristics of cirrus clouds over a southern european lidar station*, *Atmos. Chem. Phys.* **7** (2007) 5519.
- [32] S. G. Lakkis, M. Lavorato and P. O. Canziani, *Monitoring cirrus clouds with lidar in the southern hemisphere: A local study over buenos aires. I. tropopause heights*, *Atmos. Res.* **92** (2009) 18.
- [33] B. V. Hai, N. X. Tuan, D. D. Thang, N. T. Binh and D. V. Trung, *Monitoring the mixing layer over hanoi using a compact lidar system*, *Proc. The 2th Academic conference on natural science for Master and PhD students from Cambodia - Laos - Malaysia - Vietnam* (2011) 389.
- [34] J. Wang, W. Liu, C. Liu, T. Zhang, J. Liu, Z. Chen *et al.*, *The determination of aerosol distribution by a no-blind-zone scanning lidar*, *Remote Sens.* **12** (2020) 626.
- [35] L. Mei, T. Ma, Z. Zhang, R. Fei, K. Liu, Z. Gong *et al.*, *Experimental calibration of the overlap factor for the pulsed atmospheric lidar by employing a collocated scheidpflug lidar*, *Remote Sensing* **12** (2020) 1227.

- [36] Y. Sasano, H. Shimizu, N. Takeuchi and M. Okuda, *Geometrical form factor in the laser radar equation: an experimental determination*, [Appl. Opt. 18](#) (1979) 3908.
- [37] A. C. Povey, R. G. Grainger, D. M. Peters, J. L. Agnew and D. Rees, *Estimation of a lidar's overlap function and its calibration by nonlinear regression*, [Appl. Opt. 51](#) (2012) 5130.